

Adaptive Fourier modeling for quantification of tremor¹

Cameron N. Riviere^{2,a}, Stephen G. Reich^b, Nitish V. Thakor^{c,*}

^a *Department of Mechanical Engineering, Johns Hopkins University, Baltimore, MD 21218, USA*

^b *Department of Neurology, Johns Hopkins School of Medicine, Baltimore, MD 21205, USA*

^c *Department of Biomedical Engineering, Johns Hopkins School of Medicine, Baltimore, MD 21205, USA*

Received 18 October 1995; received in revised form 29 August 1996; accepted 22 October 1996

Abstract

A new computational method for quantification of tremor, the weighted frequency Fourier linear combiner (WFLC), is presented. This technique rapidly determines the frequency and amplitude of tremor by adjusting its filter weights according to a gradient search method. It provides continual tracking of frequency and amplitude modulations over the course of a test. By quantifying time-varying characteristics, the WFLC assists in correctly interpreting the results of spectral analysis, particularly for recordings exhibiting multiple spectral peaks. It therefore supplements spectral analysis, providing a more accurate picture of tremor than spectral analysis alone. The method has been incorporated into a desktop tremor measurement system to provide clinically useful analysis of tremor recorded during handwriting and drawing using a digitizing tablet. Simulated data clearly demonstrate tracking of variations in frequency and amplitude. Clinical recordings then show specific examples of quantification of time-varying aspects of tremor. © 1997 Elsevier Science B.V.

Keywords: Tremor; Handwriting; Drawing; Frequency; Fourier modeling; Modulation; Adaptive filtering

1. Introduction

Tremor is defined as a roughly sinusoidal, or oscillatory, involuntary motion (Elble and Koller, 1990). Clinical classification of tremor is based on the body parts involved, position of maximum activation, morphology, and frequency (Reich, 1995). Quantification of tremor is of clinical interest as an aid to diagnosis and to evaluate objectively the effect of treatment (Elble, 1986). Handwriting and drawing specimens are often used to examine tremor. Recording such specimens using a digitizing tablet has been introduced as one way

to provide precise quantification (Elble et al., 1990; Marquardt and Mai, 1994).

Because of its oscillatory characteristic, tremor is well suited to spectral analysis, the most popular method of tremor quantification (Wade et al., 1982; Elble and Koller, 1990). The idea is to calculate a power spectral density function indicating the signal power at different frequencies across the spectrum. The dominant frequency of tremor is evident from a visible peak in the power spectral density, while the average tremor amplitude can be determined from the area under the peak (Elble et al., 1990).

Fourier's theorem states that a periodic signal may be represented as a sum of sine and cosine waves at different harmonic frequencies, or integer multiples of the fundamental (lowest) frequency (Boyce and DiPrima, 1986). This representation, known as a Fourier series, gives rise to the Fourier transform, which transforms a signal from the time domain to the frequency domain. Most spectral analysis techniques

* Corresponding author. Present address: Department of Biomedical Engineering, Johns Hopkins University, 720 Rutland Ave., Baltimore, MD 21205, USA. Tel.: +1 410 9557093; fax: +1 410 955-054909; e-mail nthakor@bme.jhu.edu

¹ Funding provided by National Institute on Disability and Rehabilitation Research (grant number H133G30064).

² The Robotics Institute, Carnegie Mellon University, Pittsburgh, PA 15213, USA.

are based on the fast Fourier transform (FFT) (Oppenheim and Schaefer, 1989). The popularity of the FFT algorithm stems largely from its computational simplicity, allowing inexpensive implementation and rapid data analysis.

FFT-based spectral methods model the input signal as a stationary periodic signal, i.e., one whose statistical characteristics do not change with time. The finite-length input data sequence is modeled as a periodic sequence with each period identical to the input sequence length (Oppenheim and Schaefer, 1989). Yet tremor amplitude and frequency are time-varying (Elble and Koller, 1990), often making power spectra difficult to interpret (Gresty and Buckwell, 1990). Therefore it is desirable to develop models which do not assume stationarity, to provide a clearer picture of individual cases of tremor by quantifying variations in the signal over time.

Several biomedical applications have been reported for nonstationary time-frequency analysis techniques such as the short-time Fourier transform (STFT) (Jamous et al., 1992), reduced interference distributions (Wood et al., 1992; Guo et al., 1994), and the Choi–Williams distribution (Choi and Williams, 1989). The STFT is obtained by segmenting the data into short sequences assumed to be stationary. The shorter each data segment, the better the assumption of stationarity, but frequency resolution is correspondingly reduced (Cohen, 1989). This method is therefore limited by a tradeoff between time and frequency resolution. Most other time–frequency representations are based upon the construction of a joint time–frequency distribution, a function of both time and frequency (Cohen, 1989). Although these techniques are often effective in representing general time varying signals with many component frequencies (Cohen, 1989), the computational burden is often considerable.

Another recently developed quantification method is the weighted–frequency Fourier linear combiner (WFLC) (Riviere and Thakor, 1996). The WFLC, a modification of the Fourier linear combiner (Vaz and Thakor, 1989), is a simple algorithm which operates completely in the time domain. It continuously tracks changes over time in signal characteristics, such as the dominant frequency and its corresponding amplitude, and quickly provides a history of tremor frequency and amplitude for clinical evaluation. The WFLC is capable of supplementing popular spectral methods by providing additional information regarding the time-varying characteristics of the tremor. We present the WFLC for quantification of tremor, using results from simulated data and clinical patient recordings.

1.1. The weighted–frequency Fourier linear combiner

The WFLC, shown in Fig. 1, is an adaptive signal processing algorithm. As such, it exhibits time-varying, self-optimizing performance by adjusting its parameters online (Widrow and Stearns, 1985). The WFLC algorithm is a frequency-adaptive extension of the Fourier linear combiner (FLC) (Vaz and Thakor, 1989; Vaz et al., 1994). It adapts to (i.e. ‘learns’) the changing amplitude of the input using the least mean square (LMS) algorithm, a gradient descent method (Appendix A). The changing frequency of the input is learned using a modification of the LMS approach (Riviere, 1995). It can be shown that the WFLC frequency adaptation is a nonlinear phase-lock technique that compares the phase of the input at each sample with that of its reference signal, and modifies the frequency weight w_{0k} accordingly (Riviere, 1995).

Due to its adaptive capabilities, the WFLC can be used to model a quasi-periodic signal when both amplitude and frequency are unknown and time-varying. The WFLC is stated as follows:

$$x_{r_k} = \begin{cases} \sin\left(r \sum_{i=1}^k w_{0_i}\right), & 1 \leq r \leq M \\ \cos\left((r - M) \sum_{i=1}^k w_{0_i}\right), & M + 1 \leq r \leq 2M \end{cases} \quad (1a)$$

$$\varepsilon_k = s_k - \mathbf{w}_k^T \mathbf{x}_k \quad (1b)$$

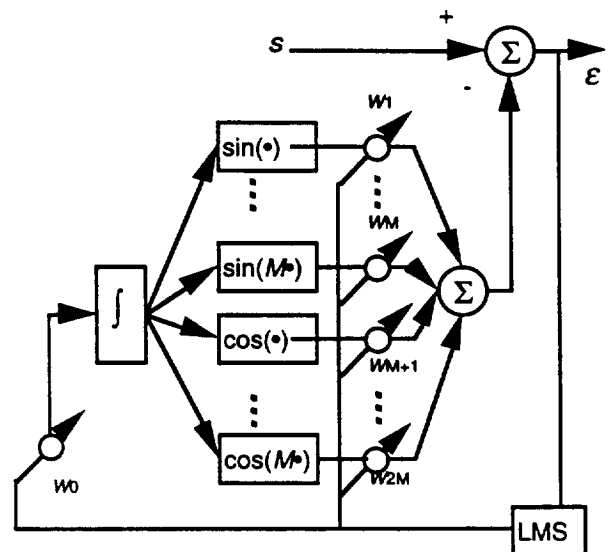


Fig. 1. Schematic of WFLC algorithm. The WFLC adaptively creates a dynamic Fourier series model of any periodic input. The vector \mathbf{x} consists of harmonic sines and cosines based on the modulated fundamental frequency ω_0 . These sinusoids are weighted by the Fourier coefficient vector \mathbf{w} and summed to provide a truncated Fourier series model of the input s . The weights ω_0 and \mathbf{w} are adapted using the LMS algorithm.

$$w_{0_{k+1}} = w_{0_k} + 2\mu_0 \varepsilon_k \sum_{r=1}^M r(w_r x_{M+r} - w_{M+r} x_r) \quad (1c)$$

$$w_{k+1} = w_k + 2\mu x_k \varepsilon_k \quad (1d)$$

where $w_k = [w_{1_k} \cdots w_{2M_k}]^T$ and $x_k = [x_{1_k} \cdots x_{2M_k}]^T$, M is the filter order, and, μ and μ_0 are the adaptive gain parameters governing convergence rates of amplitude and frequency, respectively. The WFLC models a quasi-periodic input signal as a truncated Fourier series of order, or number of harmonics, M . The WFLC may be thought of as comparing a reference oscillation with the input signal, then adjusting the frequency, amplitude, and phase of the reference oscillation until they match the input. Eq. (1a) shows the reference input vector x_k , consisting of sine and cosine waves at each of the harmonic frequencies $w_{0_k}, 2w_{0_k}, \dots, Mw_{0_k}$. This vector is the basis of the Fourier representation. The coefficients of the Fourier series model of the input are the components of the vector of amplitude adaptive weights, w_k . The running sums in Eq. (1a) preserve the phase of the frequency-modulated reference sinusoids. Eq. (1b) computes the filter error ε_k , or the difference between the primary input signal S_k and the prediction obtained from the Fourier model. Once the error is computed, the adaptive weights are then updated accordingly in the next two equations. The recursion Eq. (1c) performs the phase-lock adaptation of the reference frequency w_{0_k} . Eq. (1d) is the LMS algorithm used to estimate the amplitude coefficients, w_k , of the Fourier series. This approach can be shown to minimize the mean square of the filter error ε_k (Widrow and Stearns, 1985). The performance and limitations of the WFLC are discussed in Appendix B.

To estimate tremor amplitude, the WFLC is followed by a second linear combiner, decoupling the amplitude estimation from the frequency estimation. This involves a second set of amplitude weights, \hat{w}_k :

$$\hat{\varepsilon}_k = S_k - \hat{w}_k^T x_k \quad (3a)$$

$$\hat{w}_{k+1} = \hat{w}_k + 2\hat{\mu} x_k \hat{\varepsilon}_k \quad (3b)$$

where $\hat{w}_k = [\hat{w}_{1_k} \cdots \hat{w}_{2M_k}]^T$. This system uses the same reference vector x_k generated by the WFLC, but makes its own error computation in Eq. (3a), adjusting the weights \hat{w}_k accordingly in Eq. (3b), again via the LMS algorithm, using its own adaptive gain $\hat{\mu}$.

The system output consists of time histories of fundamental frequency and amplitude of tremor over the course of each test. The fundamental frequency f_{0_k} is obtained from the frequency weight, w_{0_k} .

$$f_{0_k} = \frac{w_{0_k}}{2\pi} \quad (4)$$

A periodogram (Kay, 1988) of the first 32 samples of s_k is used to initialize w_{0_k} . The effective tremor amplitude a_{i_k} of the i th harmonic is

$$a_{i_k} = \sqrt{\hat{w}_{i_k}^2 + \hat{w}_{M+i_k}^2} \quad (5)$$

If desired, the effective peak-to-peak tremor amplitude may be obtained by multiplying a_{i_k} by 2. For clinical use, the mean and standard deviation of the frequency and amplitude results may also be calculated.

2. Experimental methods

A SummaSketch digitizing tablet (Summagraphics, Seymour, CT) with a two-button stylus was used to collect data. The stylus resembles a pen. Digitizing tablet operation was described by Elble et al. (1990). The data sampling rate of the tablet is 116 Hz. This sampling rate avoids aliasing, since the highest frequencies of pathological hand tremor are between 12 and 15 Hz, and normal handwriting and drawing frequencies are no higher than 6 Hz (Elble et al., 1990). The resolution of the tablet is 400 lines per cm, with accuracy of ± 0.004 cm. Data for the study were transmitted in binary format to an IBM-compatible PC, via a driver written in Microsoft Quick Basic. The data were then processed by the WFLC program, written in Borland Turbo C. The tremor quantification package includes a graphics routine which presents the frequency and amplitude histories on the computer screen and printer.

To avoid biased frequency estimates from the colored voluntary motion, the data were first highpass filtered using `filtfilt`, a forward-backward filtering technique featuring zero phase shift, available in Matlab (The Math Works, Natick, MA). The filter was a 1000-order Hamming-windowed finite impulse response highpass with linear phase (designed using the Matlab command `fir1`). The cutoff frequency of 1 Hz was chosen to preserve the frequency range of pathological tremor, which is typically 2 Hz or greater (Elble and Koller, 1990). The first 2 s of each recording were set aside to allow the adaptive algorithm to learn the tremor characteristics, and therefore not included in the figures. The following parameter values were used: $\mu = 0.06$, $\mu_0 = 1.2 \times 10^{-7}$, $\hat{\mu} = 0.15$, $M = 1$. The results presented are the tremor frequency f_{0_k} and the amplitude a_{1_k} (Eqs. (4) and (5)).

To demonstrate the WFLC in a simple fashion, the technique was first tested on two synthetic data sets described below. The system was then tested using clinical data recorded as described above. The subjects were a man, age 68, with Parkinsonian tremor, and a man, age 84, with essential tremor. The essential tremor subject drew an Archimedes spiral on the digitizing tablet. He was observed to ensure that no cycle of the spiral was drawn faster than 1 Hz. The Parkinsonian subject rested the pen on the tablet. The subjects gave written consent according to a protocol approved by

the Joint Committee on Clinical Investigation of the Johns Hopkins Medical Institutions. Additional data, from a patient with advanced essential tremor, displaying spontaneous changes in frequency, was provided by Dr R.J. Elble. This patient wrote a series of cursive *l*'s on a digitizing tablet. The sampling rate for this data was 169 Hz, and, $\hat{\mu} = 0.1$ was used.

3. Synthetic data

3.1. Data set 1

The first data set was used to test tracking of large changes in tremor frequency and amplitude by the WFLC. The basic model used to simulate tremor was similar to that of Gresty and Buckwell (1990):

$$\tau_k = K(1 + n_{a_k}) \cos(2\pi f k + b n_{f_k}), \quad (6)$$

incorporating bandwidth limited noise components, n_a and n_f , filtered -20 dB down at 1.2 Hz. The noise magnitudes were limited to avoid phase reversal. The Gresty and Buckwell model was expanded to also include deterministic components, ξ_a and ξ_f , which modulated the signal amplitude and frequency. The tremor signal was therefore simulated in the following way:

$$s_k = K(1 + n_{a_k} + \xi_{a_k}) \cos(2\pi f k + b n_{f_k} + \xi_{f_k}). \quad (7)$$

The parameters used were: $K = 0.56$ cm, $f = 3$ Hz, and $b = 0.15$. ξ_f modulated the carrier frequency to approximately 5 Hz by the end of the data set.

For data set 1, the frequency error, or difference between the true frequency and WFLC frequency estimate, was

$$\tilde{f}_k = f + \frac{b}{2\pi} \frac{dn_{f_k}}{dk} + \frac{1}{2\pi} \frac{d\xi_{f_k}}{dk} - \frac{w_{0k}}{2\pi}. \quad (8)$$

The error between the WFLC frequency estimate and the deterministic part of the input frequency was

$$\tilde{f}_{d_k} = \left(f + \frac{1}{2\pi} \frac{d\xi_{f_k}}{dk} \right) - \frac{w_{0k}}{2\pi}. \quad (9)$$

The amplitude error was

$$\tilde{a}_k = a_{1_k} - K(1 + n_{a_k} + \xi_{a_k}), \quad (10)$$

with deterministic component

$$\tilde{a}_{d_k} = a_{1_k} - K(1 + \xi_{a_k}). \quad (11)$$

3.2. Data set 2

The purpose of the second data set was to test the behavior of the WFLC when multiple tremor frequencies were present. Two separate tremor signals were generated according to the Gresty and Buckwell (1990) model (6), at $f = 3$ Hz and $f = 5$ Hz, respectively. The

following parameters were used: $K = 0.42$ cm, $b = 0.15$. These were then added to produce data set 2, containing two simultaneous oscillations: $s_k = \tau_k \{3 \text{ Hz}\} + \tau_k \{5 \text{ Hz}\}$. The duration of each synthetic data set was 60 s.

4. Results

4.1. Synthetic data

Results for synthetic data set 1 are presented in Fig. 2. The WFLC signal model clearly tracked the signal frequency as it modulated from 3 to 5 Hz. The mean frequency error was -0.007 Hz. The algorithm also modeled the amplitude-modulating effects of both the noise n_a and the deterministic component ξ_a , with mean amplitude error of 0.2% of the average input amplitude. The error values are summarized in Table 1.

The results for synthetic data set 2, shown in Fig. 3, demonstrate the behavior of the system when two sinusoids of roughly equal power are present, as shown in the spectral density of Fig. 3(d). The WFLC is designed to model a single oscillation, whose frequency may be modulating (Section 2). For data set 2 the error gradient had a local minimum at each of the two sinusoids, and since they had approximately equal power, the WFLC converged to the frequency nearest its initial value. As Fig. 3(b) shows, the algorithm tended to the lower frequency of the two sinusoids. The WFLC results in Fig. 3(b) do not reflect any modulation of the signal from 3–5 Hz during the test. Since the two frequencies in question are not harmonics, this indicates that the multiple peaks in the spectrum of Fig. 3(d) are due to independent simultaneous oscillations.

Note the similarity between the power spectral densities in Fig. 2(d), and Fig. 3(d), despite the large difference in the actual signals. Despite their similar power spectra, the WFLC distinguished between the two signals, data sets 1 and 2, by displaying their time-varying frequency characteristics in Fig. 2(b) and Fig. 3(b).

4.2. Patient recordings

Figs. 4–6 present clinical examples of tremor quantified using the WFLC. The subject with Parkinsonian tremor produced the results shown in Fig. 4. As is common in Parkinsonian tremor (Lakie and Mutch, 1989), this recording shows almost no frequency modulation. The algorithm identified the tremor frequency of ≈ 4 Hz, as reflected in Fig. 4(b).

Results from the first subject with essential tremor are displayed in Fig. 5. As shown in Fig. 5(d), this recording exhibited two prominent spectral peaks at 1.50 and 5.00 Hz. The latter frequency is not a harmonic, or multiple, of the former. Since the WFLC is

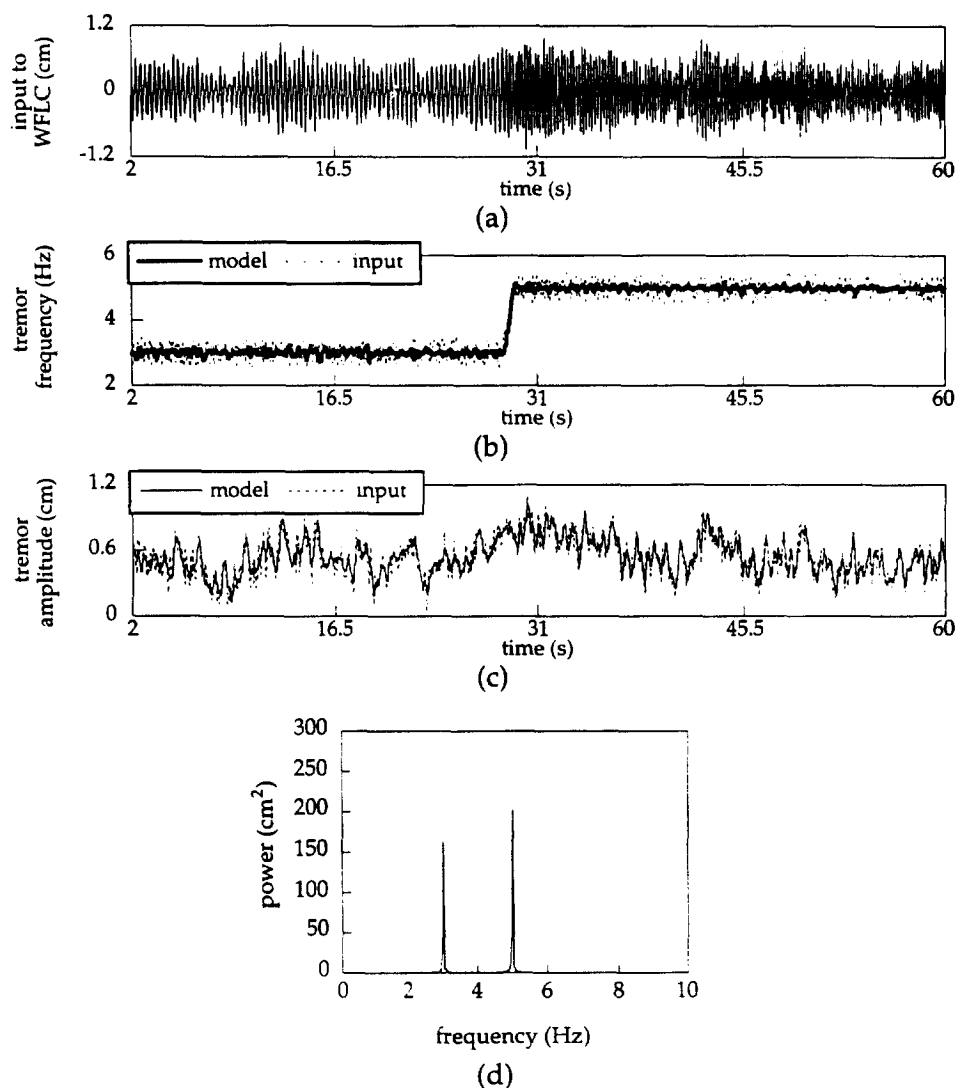


Fig. 2. Results for synthetic data set 1. Carrier frequency changes from 3 to 5 Hz during the test. (a) High-pass filtered input to WFLC. (b) Frequency results. Mean = 4.1 Hz, S.D. = 1.0 Hz. (c) Amplitude results. Mean = 0.54 cm, S.D. = 0.16 cm. (d) Power spectral density via FFT.

designed to model a single nonstationary oscillation, the frequency weight tracks the single dominant frequency at each step. It therefore clarifies, in Fig. 5(b),

Table 1
WFLC frequency and amplitude error for simulated tremor (data set I, Fig. 2)

Parameter	Mean Error	S.D
Frequency (Hz)		
Overall	-0.007	0.275
Deterministic component	-0.007	0.076
Amplitude (% of input)		
Overall	0.2	12.7
Deterministic component	-3.5	21.2

Amplitude error is presented as a percentage of the average input amplitude.

that in this test the spectral peak at 5 Hz is not due to modulation of the lower frequency oscillation during the test, but rather to a separate oscillation. If a modulation to 5 Hz had occurred, it would be reflected in the WFLC frequency results, as in Fig. 2(b).

Fig. 6 presents results from a patient with advanced essential tremor. In some severe cases essential tremor has been found to exhibit unusual spontaneous frequency modulations (Elble and Koller, 1990), as Fig. 6(a) shows. These modulations are reflected in the WFLC frequency results in Fig. 6(b). The power spectrum exhibits numerous peaks from 1.5 to 8.5 Hz. The frequency history in Fig. 6(b) covers almost this entire range, suggesting that the multiple spectral peaks are due to frequency modulation of the tremor during the test, rather than to multiple simultaneous oscillations.

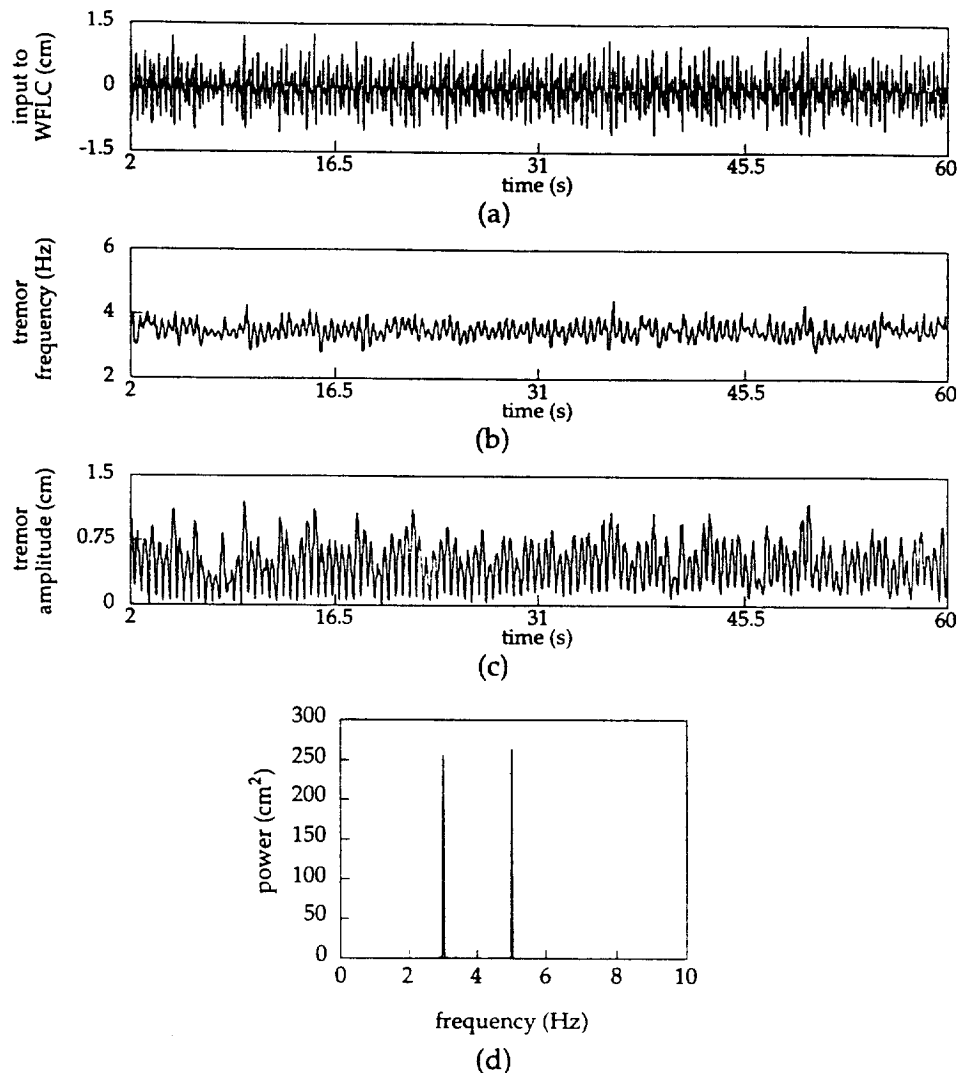


Fig. 3. Results for synthetic data set 2. This set consists of two simultaneous sine waves: one at 3 Hz and one at 5 Hz. (a) High-pass filtered input to WFLC. (b) Frequency results. Mean = 35 Hz, S.D. = 0.2 Hz. (c) Amplitude results. Mean = 0.49 cm, S.D. = 0.24 cm. (d) Power spectral density via FFT.

5. Discussion

Existing quantitative methods for signal analysis include the FFT, STFT, autoregressive (AR) estimators, wavelet transforms, and time–frequency (t – f) distributions. The FFT and STFT are limited by a tradeoff in resolution between time and frequency (Cohen, 1989). The FFT and AR methods are not suited to nonstationarity. AR estimators offer high frequency resolution, but depend on a priori knowledge of model order, which is difficult to obtain. Too large a model order can cause spurious spectral peaks (Kay, 1988). Wavelet analysis, decomposing a signal onto basis functions, offers good time resolution at high frequencies, and good frequency resolution at low frequencies (Mallat, 1989). It handles nonstationarity, but depends upon prior selection of a proper wavelet prototype. The current theory provides no clear answer as to what

family of wavelets is best for a given application. T – f distributions represent nonstationary signals, but can exhibit spurious spectral content due to cross terms (Cohen, 1989).

The WFLC possesses a number of beneficial characteristics. It is computationally simple, operates in the time domain, offers high resolution, and is well suited to nonstationary spectral analysis, explicitly presenting variations in frequency and amplitude. As a real-time tracking algorithm, the WFLC requires some time to adapt to changes in signal characteristics, converging according to Eq. (B-1) and Eq. (B-2). It cannot respond instantaneously to changes in the input; however, it does not suffer from cross terms.

Unlike most other methods, the WFLC is designed to represent only a single nonstationary oscillation. This simplifies clinical interpretation, as often only one oscillation of interest is present. However, when multi-

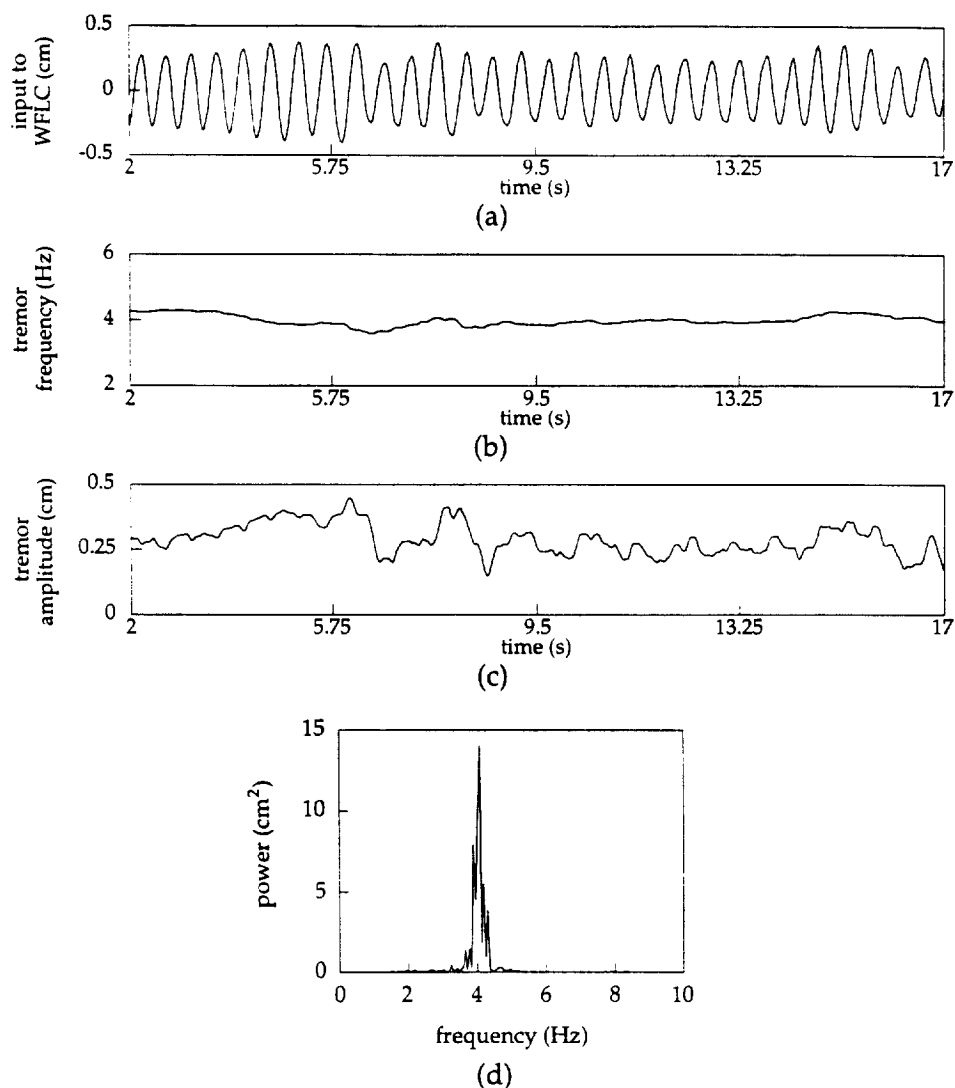


Fig. 4. Sample from patient with Parkinsonian tremor. Subject rested pen on tablet. (a) High-pass filtered input to WFLC. (b) Frequency results. Mean = 4.0 Hz, S.D. = 0.1 Hz. (c) Amplitude results. Mean = 0.23 cm, S.D. = 0.08 cm. (d) Power spectral density via FFT.

ple oscillators are present, the WFLC cannot model both. Oscillations other than the primary one identified by the WFLC can be seen in the suggested companion FFT, as presented in each of the data figures. Alternatively, if the number of oscillations present is known, multiple WFLCs may be initialized at different frequencies, and allowed to track the multiple independent oscillations. If two oscillations are close in frequency, small μ_0 values should be used, and a long duration will be needed for convergence.

The WFLC is an adaptive signal processing technique that learns input signal characteristics over time. The rate of adaptation can be modified easily by changing the adaptive gain parameters of the filter. High adaptive gains offer faster convergence and better tracking of modulation of tremor frequency and amplitude, but produce greater susceptibility to noise and artifacts. Low adaptive gains are less susceptible

to noise, but also less capable of tracking signal modulation. If rapid tracking of signal modulation is desired, care should be taken to avoid voluntary motion in the frequency range of tremor, e.g. by ensuring an Archimedes spiral is drawn slowly.

Slow amplitude modulation is present in some cases of tremor. This produces a low spectral sideband, but the slow amplitude change is likely to be lost with the highpass prefilter used in these experiments. If detection of such a sideband in the WFLC results is desired, careful restriction of the voluntary motion will allow the use of a much lower prefilter cutoff frequency, preserving the slow oscillation in the amplitude weights (part (c) of each figure). Parkinsonian resting tremor often exhibits this sort of slow amplitude modulation. Since voluntary motion is zero by definition in this case, the highpass prefilter may be omitted altogether.

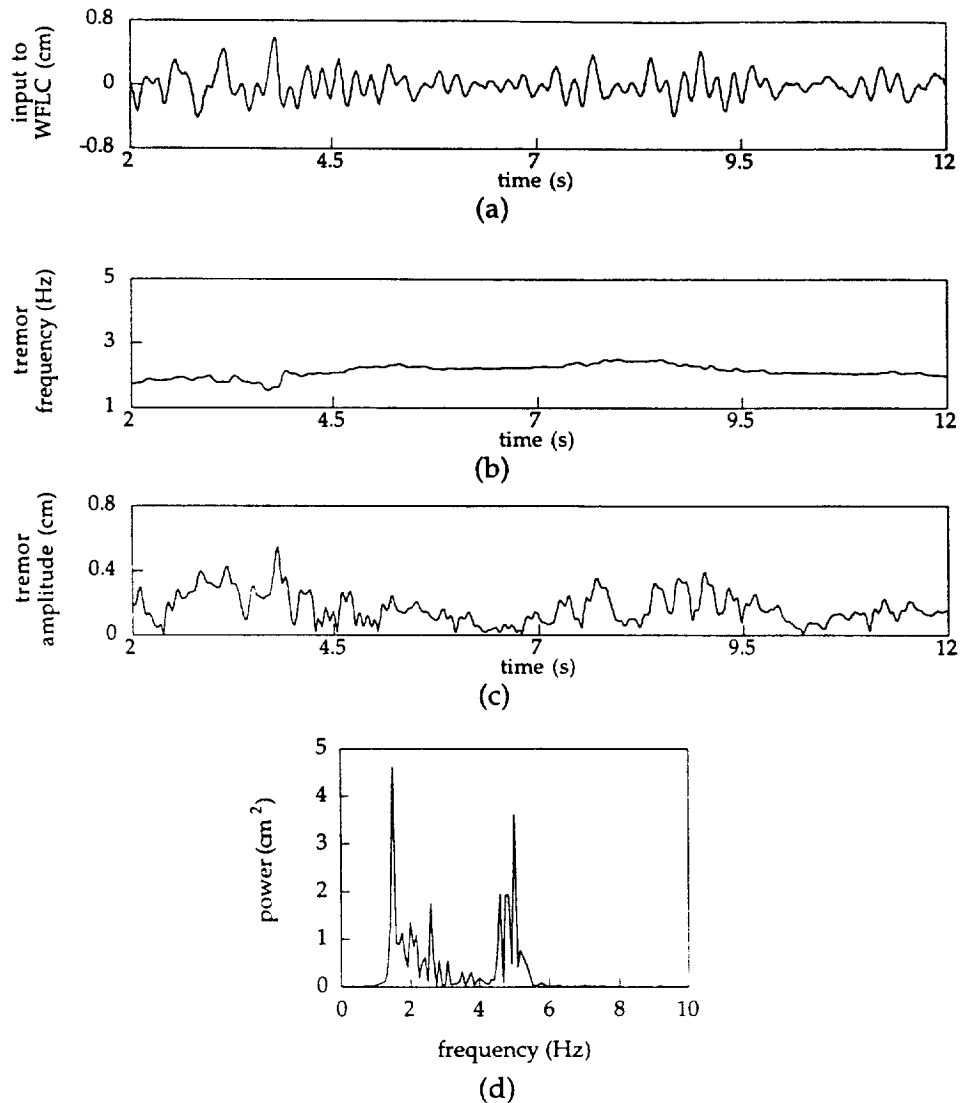


Fig. 5. Sample from male patient with essential tremor. Subject drew an Archimedes spiral. (a) High-pass filtered input to WFLC. (b) Frequency results. Mean = 2.1 Hz, S.D. = 0.2 Hz. (c) Amplitude results. Mean = 0.17 cm, S.D. = 0.10 cm. (d) Power spectral density via FFT.

While the present work analyzes displacement data obtained with a digitizing tablet, the WFLC is equally suited to processing tremor recordings from other sources, such as accelerometers, and of other quantities, such as velocity and acceleration. The algorithm is computationally simple, and provides clinical results rapidly. Because it continuously tracks changes in tremor frequency and amplitude, the WFLC is well suited to processing long term recordings (Tyrer and Bond, 1974; Redmond and Hegge, 1985). It can also be used in real time as a rehabilitative tremor-reducing aid for computer input using a mouse, digitizing tablet, or pen interface (Riviere and Thakor, 1996).

Temporal variation in tremor frequency often takes the form of frequency modulation, or 'jitter,' around a constant 'carrier frequency' (Gresty and Buckwell, 1990), but sometimes includes larger frequency modulation, which might be described as a change in the

carrier frequency itself. An extreme example of the latter is presented in Elble et al. (1990), in which the tremor frequency changes spontaneously from ≈ 4.2 to 7.2 Hz. The WFLC is designed to track changes in carrier frequency, rather than rapid jitter about the carrier frequency. This characteristic is exemplified by the standard deviation of the frequency error from simulated data set 1 (Table 1). The capability of the WFLC to detect changes in frequency is demonstrated via simulation in Fig. 2(b). Another example of this can be seen in Fig. 6, where the dominant tremor frequency is rapidly changing. FFT-based spectral analysis of tremor reflects the presence of multiple frequency components (Fig. 2(d), Fig. 3(d), Fig. 5(d) and Fig. 6(d)), but it does not indicate the frequency variation over time in the signal (Cohen, 1989), whereas the WFLC quantifies this frequency modulation (Fig. 2(b) and Fig. 6(b)), or the lack of it (Fig. 3(b) and Fig. 5(b)). Sub-

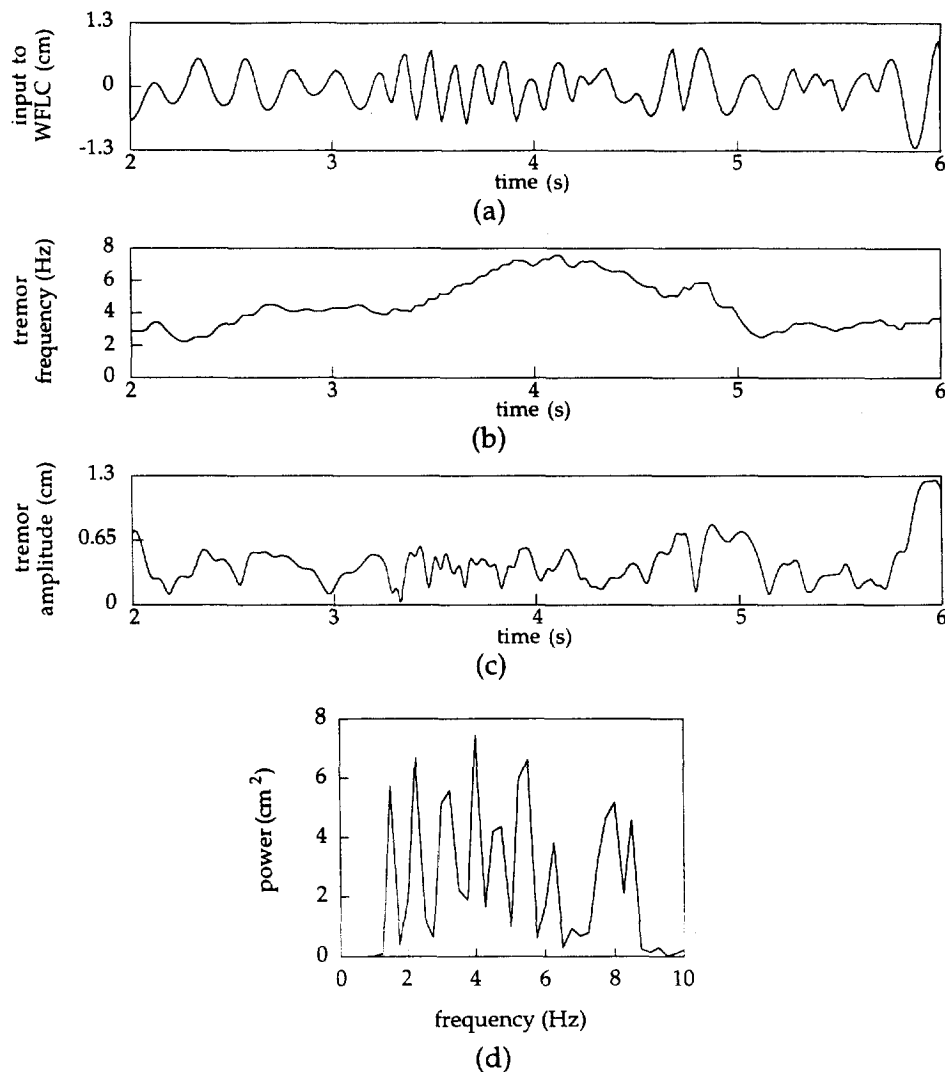


Fig. 6. Sample from patient with advanced essential tremor. Subject drew a series of cursive *l*'s. (a) High-pass filtered input to WFLC. (b) Frequency results. Mean = 4.5 Hz, S.D. = 1.5 Hz. (c) Amplitude results. Mean = 0.42 cm, S.D. = 0.22 cm. (d) Power spectral density via FFT.

stantial changes in tremor frequency during brief recordings are somewhat rare (Riley and Rosen, 1987) (e.g. Fig. 4). Therefore, the larger the standard deviation of the WFLC frequency output, the more likely the tremor is either a relatively unusual case containing multiple oscillations or more rapid modulation, as in Fig. 6, or possibly multiple oscillations whose amplitudes vary such that none are consistently dominant.

The WFLC is particularly useful when spectral analysis of tremor exhibits multiple peaks. The presence of multiple spectral peaks has sometimes been interpreted to indicate the presence of multiple independent tremor mechanisms (Findley et al., 1981). Gresty and Buckwell (1990) pointed out that this is often done in error, since multiple peaks may be due to modulation of a single tremor mechanism. Fourier analysis decomposes a signal into individual frequency components, but it does not indicate when a given frequency occurred (Cohen, 1989). Signals strongly different in time may exhibit

almost identical power spectra. As seen in Fig. 2(d) and Fig. 3(d), a single oscillation modulating from one frequency to another is difficult to distinguish from two independent oscillations solely on the basis of spectral analysis. By quantifying the time-varying characteristics of the tremor signal, the WFLC correctly interprets the results of spectral analysis. Combining the WFLC with the FFT for analysis of tremor provides not only a power spectrum, but also graphical and statistical information about variations in tremor frequency and amplitude, producing a more accurate picture of tremor than the FFT alone.

Acknowledgements

The authors are happy to provide the source code for the WFLC algorithm. This may be requested via e-mail at cam.riviere@cmu.edu or from the corresponding au-

thor. This work was supported by grant H133G30064 from the National Institute on Disability and Rehabilitation Research. The authors are grateful to Dr R.J. Elble of Southern Illinois University for providing data from subjects with advanced essential tremor. The authors also thank Y. Sun and M. Kim for data analysis.

Appendix A. The Least-mean-square Algorithm

The least-mean-square (LMS) algorithm (Widrow and Stearns, 1985) is a simple adaptive signal processing method. It is most commonly used in an ‘adaptive linear combiner’ architecture, so named because the filter output is a linear combination of the reference inputs. The LMS algorithm is an iterative gradient search method, which adjusts its filter weights at each time step to optimize its performance. Given a desired response s_k and a reference input vector \mathbf{x}_k composed of signals x_{1k}, \dots, x_{2M_k} , the filter error is

$$\varepsilon_k = s_k - \mathbf{w}_k^T \mathbf{x}_k \quad (\text{A-1})$$

Holding the weights constant and assuming s_k , \mathbf{x}_k , and ε_k wide sense stationary, the mean square error (MSE) is

$$\xi = E[\varepsilon_k^2] = E[s_k^2] + \mathbf{w}^T \mathbf{R} \mathbf{w} - 2E[s_k \mathbf{x}_k^T] \mathbf{w} \quad (\text{A-2})$$

where $E[\cdot]$ denotes expected value, and $\mathbf{R} = E[\mathbf{x}_k \mathbf{x}_k^T]$. The MSE ξ is minimized at the point where its gradient is zero:

$$\frac{\partial \xi}{\partial \mathbf{w}} = 2\mathbf{R} \mathbf{w} - 2E[s_k \mathbf{x}_k] = 0 \quad (\text{A-3})$$

The optimum weight vector \mathbf{w}^* , which results in the minimum error, is then $\mathbf{w}^* = \mathbf{R}^{-1} E[s_k \mathbf{x}_k]$. This vector, not known a priori, is the goal of the iterative gradient search.

The gradient search method commonly used is a steepest descent approach, in which the weights are adjusted in the decreasing direction of the gradient:

$$\mathbf{w}_{k+1} = \mathbf{w}_k - \mu \frac{\partial \xi_k}{\partial \mathbf{w}_k}$$

The LMS algorithm simplifies the gradient search by using the instantaneous squared error ε_k^2 as an estimate of ξ . The LMS gradient search iteration which adjusts the filter weights is then

$$\mathbf{w}_{k+1} = \mathbf{w}_k - \mu \frac{\partial \varepsilon_k^2}{\partial \mathbf{w}_k} \quad (\text{A-4})$$

which from (A-1) is

$$\mathbf{w}_{k+1} = \mathbf{w}_k + 2\mu \varepsilon_k \mathbf{x}_k \quad (\text{A-5})$$

The LMS algorithm can be shown to be stable for (Widrow and Stearns, 1985)

$$0 < \mu < \frac{1}{\text{tr}[\mathbf{R}]} \quad (\text{A-6})$$

where $\text{tr}[\cdot]$ indicates the matrix trace.

Appendix B. Performance of the WFLC

The frequency adaptation of the WFLC uses a non-linear phase-lock technique (Viterbi, 1966), hence it is not possible to define a time constant for frequency adaptation. In the absence of noise, the frequency convergence behavior of the algorithm is described approximately by the following expression for the change in the frequency weight w_{0k} at time k (Riviere, 1995):

$$w_{0k+1} - w_{0k} = \frac{2\mu_0 \mu p}{\sqrt{\mu^2 + \tilde{w}_{0k}^2}} \sin\left(\tan^{-1}\left(\frac{\tilde{w}_{0k}}{\mu}\right)\right) \quad (\text{B-1})$$

where, μ_0 and μ are the adaptive gains for frequency and amplitude, respectively, p is the power of the input oscillation being modeled, and \tilde{w}_{0k} is the error, or difference, in frequency between the input oscillation and the WFLC model at time k . Assuming frequency convergence, the convergence time constant for the amplitude weights, \mathbf{w}_k , is (Vaz and Thakor, 1989):

$$\tau_e = \frac{1}{2\mu} \quad (\text{B-2})$$

The same holds for $\hat{\mathbf{w}}_k$, with $\hat{\mu}$ substituted for μ .

The ability of the WFLC to respond to rapid frequency shifts therefore depends upon the selected adaptive gain parameters, the input power, and the frequency error, or size of the shift (B1). Detection of oscillation components requires sufficient duration for convergence to occur. The frequency convergence behavior of the WFLC can be seen in Fig. 6(b) in the frequency increase from roughly 4–7.5 Hz between 3.5 and 4 s. The frequency convergence rate can be increased by increasing μ_0 , but should be kept well below $2/p$, where p is the input power (Riviere, 1995). As an adaptive modeling algorithm, once convergence occurs, WFLC results are independent of data record length for stationary input.

References

- Boyce, W. and DiPrima, R. (1986) Elementary Differential Equations and Boundary Value Problems, Wiley, New York, 654 pp.
- Choi, H.I. and Williams, W.J. (1989) Improved time–frequency representation of multicomponent signals using exponential kernels, IEEE Trans. Acoust. Speech Signal Process, 37: 862–871.
- Cohen, L. (1989) Time-frequency distributions—a review, Proc. IEEE, 77: 941–981.
- Elble, R.J. (1986) Physiologic and essential tremor, Neurology, 36: 225–231.

- Elble, R.J., Sinha, R. and Higgins, C. (1990) Quantification of tremor with a digitizing tablet, *J. Neurosci. Methods*, 32: 193–198.
- Elble, R.J. and Koller, W.C. (1990) Tremor, Johns Hopkins University Press, Baltimore, 204 pp.
- Findley, L.J., Gresty M.A. and Halmagyi GM. (1981) Tremor, the cogwheel phenomenon and clonus in Parkinson's disease, *J. Neurol. Neurosurg. Psychiatry.*, 44: 534–546.
- Gresty, M. and Buckwell, D. (1990) Spectral analysis of tremor understanding the results, *Electroencephalogr. Clin. Neurophysiol.*, 53: 976–981.
- Guo, Z., Durand, L.-G. and Lee, H.C. (1994) Comparison of time–frequency distribution techniques for analysis of simulated Doppler ultrasound signals of the femoral artery, *IEEE Trans. Biomed. Eng.*, 41: 332–342.
- Jamous, G., Durand, L.-G., Langlois, Y.E., Lanthier, T., Pibarot, P. and Carioto, S. (1992) Optimal time-window duration for computing time/frequency representations of normal phonocardiograms in dogs, *Med. Biol. Eng. Comput.*, 30: 503–508.
- Kay, S. (1988) *Modern Spectral Estimation*, Prentice Hall, Englewood Cliffs, N.J., 543 pp.
- Lakie, M. and Mutch, W.J. (1989) Finger tremor in Parkinson's disease, *J. Neurol. Neurosurg. Psychiatry*, 52: 392–394.
- Mallat, S.G. (1989) A theory of multiresolution signal decomposition: the wavelet representation, *IEEE Trans. Pattern Anal. Mach. Intell.*, 2: 674–693.
- Marquardt, C. and Mai N. (1994) A computational procedure for movement analysis in handwriting, *J Neurosci. Methods*, 52: 39–45.
- Oppenheim, A.V. and Schaefer, R.W. (1989) *Discrete-Time Signal Processing*, Prentice Hall, Englewood Cliffs, N.J., 879 pp.
- Redmond, D.P. and Hegge, F.N. (1985) Observations on the design and specification of a wrist-worn activity monitoring system, *Behav. Res. Methods Inst. Comput.*, 17: 659–669.
- Reich, S.G. (1995) Common disorders of movement tremor and Parkinson's Disease. In L.R. Barker, J.R. Burton, and P.D. Zieve (Eds.), *Principles of Ambulatory Medicine*, fourth edition, Williams and Wilkins, Baltimore, pp. 1217–1229.
- Riley, P.O. and Rosen, M.J. (1987) Evaluating manual control devices for those with tremor disability, *J. Rehab. Res. Dev.*, 24: 99–110.
- Riviere, C.N. (1995) Adaptive suppression of tremor for improved human-machine control, Ph.D. dissertation, Johns Hopkins University, Baltimore, MD.
- Riviere, C.N. and Thakor, N.V. (1996) Modeling and canceling tremor in human-machine interfaces, *IEEE Eng. Med. Biol. Mag.*, 15(3): 29–36.
- Tyrer, P.J. and Bond, A.J. (1974) Diurnal variation in physiological tremor, *Electroencephalogr. Clin. Neurophysiol.*, 37: 35–40.
- Vaz, C.A. and Thakor, N.V. (1989) Adaptive Fourier estimation of time varying evoked potentials, *IEEE Trans. Biomed. Eng.*, 36: 448–455.
- Vaz, C., Kong, X. and Thakor, N. (1994) An adaptive estimation of periodic signals using a Fourier Linear Combiner, *IEEE Trans. Signal Process.*, 42: 1–10.
- Viterbi, A.J. (1966) *Principles of Coherent Communication*, McGraw-Hill, New York, 321 pp.
- Wade, P., Gresty, M.A. and Findley, L.J. (1982) A normative study of postural tremor of the hand, *Arch. Neurol.*, 39: 358–362.
- Widrow, B. and Stearns, S.D. (1985) *Adaptive Signal Processing*, Prentice-Hall, Englewood Cliffs, N.J., 474 pp.
- Wood, J.C., Buda, A.J. and Barry, D.T. (1992) Time–frequency transforms: a new approach to first heart sound frequency analysis, *IEEE Trans. Biomed. Eng.*, 39: 728–739.